Correspondence

A Piezoelectric Energy Harvester With Increased Bandwidth Based on Beam Flexural Vibrations in Perpendicular Directions

Peng Li, Feng Jin, and Jiashi Yang

***Abstract*—We propose a new structure for piezoelectric energy harvesters. It consists of an elastic beam with two pairs of piezoelectric films operating with the fundamental flexural modes in perpendicular directions. A one-dimensional model is developed and used to analyze the proposed structure. The output power density is calculated and examined. Results show that, with simultaneous flexural motions in two perpendicular directions, the output power has two peaks close to each other resulting from the two fundamental flexural resonances. The distance between the two peaks can be adjusted through design to make the two peaks merge into one wide peak. Hence, the frequency bandwidth through which energy can be harvested is roughly doubled when compared with conventional beam bimorph energy harvesters operating with flexural motion in one direction and one resonance only.**

I. Introduction

Piezoelectric materials are natural candidates for power or energy harvesters that scavenge ambient vibration energy by converting mechanical energy into electrical energy, which is then used for powering wireless electronic devices with a low power requirement [1]–[7]. More references can be found in a review article [8]. Ambient mechanical vibration energy may have various frequency spectra. A piezoelectric power harvester is a resonant device [6] in the sense that its electrical output is highly frequency dependent and is relatively large only near a particular resonant frequency of the harvester structure. Therefore, a specific power harvester can effectively pick up ambient vibration energy only at or near a particular frequency. Although power harvesters of different frequencies can be designed, their resonances are all narrowband, in the sense that they can only collect energy effectively near a particular resonant frequency. Recently, there have been increasing efforts to develop broadband energy harvesters which can harvest energy over a finite frequency interval [9]–[11]. Typically, this is achieved by electrically and/or mechanically connecting a few energy harvesters whose operating frequencies are slightly different and are very close to each other. In this paper, we propose a different structural design of an energy harvester with an increased bandwidth operating with the two flexural modes in perpendicular directions of a single beam. It is shown through a theoretical analysis that the proposed structure can pick up vibration energy over a frequency range which is about twice the bandwidth of a typical single-beam harvester structure in flexural motion in one direction only.

Manuscript received February 4, 2013; accepted July 12, 2013. The National Natural Science Foundation of China (number 11272247), the National 111 Project of China (number B06024), and the Scholarship Award for Excellent Doctoral Student granted by the Ministry of Education are gratefully acknowledged for their financial support. This work was also partially supported by the U.S. Army Research Office (grant number W911NF-10-1-0293).

P. Li and F. Jin are with the State Key Laboratory for Mechanical Structure, Strength, and Vibration, School of Aerospace, Xi'an Jiaotong University, Xi'an, China (e-mail: jinfengzhao@263.net).

J. Yang is with the Department of Mechanical and Materials Engineering, University of Nebraska-Lincoln, Lincoln, NE (e-mail: jyang1@unl.edu).

DOI http://dx.doi.org/10.1109/TUFFC.2013.2813

II. Structure

Consider the beam shown in Fig. 1(a). The left end of the beam is cantilevered into a wall that is in a vertical, time-harmonic motion with a known amplitude A at a given frequency ω. The right end of the beam is connected to a concentrated mass. The concentrated mass is made from a heavy material. Its mass must be considered, but it is geometrically small so that its rotatory inertia can be neglected [7]. Fig. 1(b) shows the cross section of the beam. It is rectangular, with b and c slightly different. Its orientation is described by θ. There are four piezoelectric ceramic films (A, B, C, and D) poled in their thickness directions. The films are electroded, with the electrodes shown by the thick lines in the figure. The bottom or inner electrodes of the films at the interface between the films and the beam are shorted and grounded as a reference. The top or outer electrodes on the films are connected to an output circuit. Effectively, the structure is like two conventional beam bimorph piezoelectric energy harvesters combined into one. The main purpose of this paper is to show that the beam can operate as an energy harvester with an increased bandwidth. Therefore, we considered the simplest situation of the output circuit which has an impedance Z_L in harmonic motions. The x_2- and x_3-axes are the centroidal principal axes. When the left end of the beam is excited by a vertical vibration, from the structural mechanics point of view, the beam motion can be broken into flexural vibrations in both of the x_2- and x_3-directions. An output voltage denoted by $4V$ is then produced. It is expected that by adjusting b and c, the frequencies of the flexural modes in the x_2 and x_3 directions can be made as close as desired. Then, the bandwidth of the electrical output may be about twice the bandwidth obtained when the beam is vibrating in the x_2- or x_3-direction only, like a conventional bimorph energy harvester [7]. This type of increased bandwidth resulting from two modes with resonant frequencies close to each other has been seen in similar structures operating with similar modes for piezoelectric gyroscope applications [12].

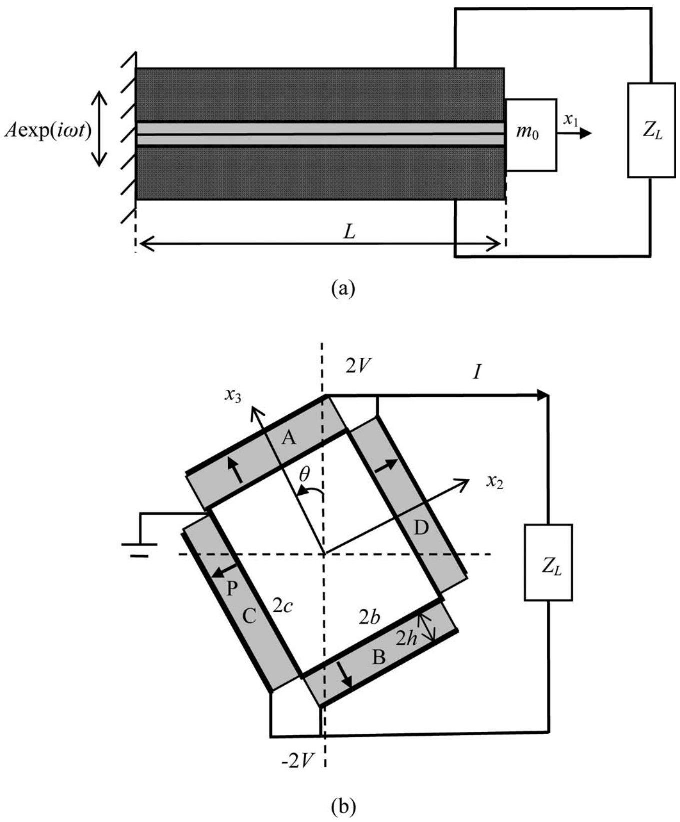

Fig. 1. A beam piezoelectric energy harvester: (a) side view and (b) cross section.

III. Governing Equations

Consider simultaneous flexural motions of the beam in the x_2- and x_3-directions with flexural displacements $u_2(x_1, t)$ and $u_3(x_1, t)$. The axial normal strain for the beam in the classical theory of flexure is [12]–[14]

$$S_1 = -x_2 u_{2,11} - x_3 u_{3,11}, \tag{1}$$

where $u_{2,11}$ and $u_{3,11}$ are the bending curvatures in the x_2- and x_3-directions. The electric fields in the piezoelectric films along their individual poling directions, indicated by P in Fig. 1(b), are denoted by E_3 and are given by [12]

$$E_3 = \begin{cases} -V/h, & \text{A and D,} \\ V/h, & \text{B and C.} \end{cases} \tag{2}$$

For beam bending, the state of stress is one-dimensional with one nonzero stress component T_1. The constitutive relations for the piezoelectric films are

$$\begin{aligned} S_1 &= s_{11}T_1 + d_{31}E_3, \\ D_3 &= d_{31}T_1 + \varepsilon_{33}E_3. \end{aligned} \tag{3}$$

s_{11}, d_{31}, and ε_{33} are the elastic, piezoelectric, and dielectric constants, respectively. We invert (3) for stress in terms of strain and substitute from (1) for the strain. This yields

$$\begin{aligned} T_1 &= s_{11}^{-1}(-x_2u_{2,11} - x_3u_{3,11}) - s_{11}^{-1}d_{31}E_3, \\ D_3 &= s_{11}^{-1}d_{31}(-x_2u_{2,11} - x_3u_{3,11}) + \bar{\varepsilon}_{33}E_3, \end{aligned} \tag{4}$$

where $\bar{\varepsilon}_{33} = \varepsilon_{33}(1 - k_{31}^2)$ and $k_{31}^2 = d_{31}^2/(\varepsilon_{33}s_{11})$. The constitutive relation for the isotropic elastic beam is simply

$$T_1 = ES_1 = -E(x_2u_{2,11} + x_3u_{3,11}). \tag{5}$$

E is the Young's modulus of the material. The bending moments for flexural motions in the x_2- and x_3-directions are defined by the following integrals over the cross-sectional area S:

$$\begin{aligned} M_2 &= \int_S x_2T_1 \mathrm{d}A = -D_{22}u_{2,11} + G_2V, \\ M_3 &= \int_S x_3T_1 \mathrm{d}A = -D_{33}u_{3,11} + G_3V. \end{aligned} \tag{6}$$

In (6),

$$\begin{aligned} D_{22} &= \frac{4}{3}Eb^3c + \frac{8}{3}s_{11}^{-1}b^3h + \frac{4}{3}s_{11}^{-1}[(b+2h)^3 - b^3]c, \\ D_{33} &= \frac{4}{3}Ec^3b + \frac{8}{3}s_{11}^{-1}c^3h + \frac{4}{3}s_{11}^{-1}[(c+2h)^3 - c^3]b, \\ G_2 &= 8s_{11}^{-1}d_{31}(b+h)c, \\ G_3 &= 8s_{11}^{-1}d_{31}(c+h)b. \end{aligned} \tag{7}$$

In the special case in which $b = c$, from (7), we have $D_{22} = D_{33}$ and $G_2 = G_3$, and they become the same as the D and G in [12, Eq. (9)] when the parameters $a = b$ in [12]. This serves as a partial verification of (6). The equations of motion for classical flexure are [12], [13]

$$\begin{aligned} M_{2,11} &= m\ddot{u}_2, \\ M_{3,11} &= m\ddot{u}_3, \end{aligned} \tag{8}$$

where $m = 4bc\rho + 8(b + c)h\rho'$ is the mass per unit length of the beam and the films together. ρ and ρ' are the mass densities of the elastic beam and the piezoelectric films, respectively. The boundary conditions at the left end, where $x_1 = 0$, are

$$\begin{aligned} u_2 &= A\sin\theta\exp(i\omega t), \quad u_{2,1} = 0, \\ u_3 &= A\cos\theta\exp(i\omega t), \quad u_{3,1} = 0. \end{aligned} \tag{9}$$

At the right end, where $x_1 = L$, we have

$$\begin{aligned} M_2 &= 0, \quad m_0\ddot{u}_2 = -M_{2,1}, \\ M_3 &= 0, \quad m_0\ddot{u}_3 = -M_{3,1}. \end{aligned} \tag{10}$$

The electric charges on the outer electrodes of the films at A and D are given by

$$\begin{aligned} Q_{\mathrm{A}} &= -\int_0^L \mathrm{d}x_1 \int_{-b}^{b} D_3(x_3 = c + 2h)\mathrm{d}x_2 \\ &= 2s_{11}^{-1}d_{31}b(c+2h)[u_{3,1}(L) - u_{3,1}(0)] + 2\bar{\varepsilon}_{33}\frac{V}{h}bL, \\ Q_{\mathrm{D}} &= -\int_0^L \mathrm{d}x_1 \int_{-c}^{c} D_3(x_2 = b + 2h)\mathrm{d}x_3 \\ &= 2s_{11}^{-1}d_{31}c(b+2h)[u_{2,1}(L) - u_{2,1}(0)] + 2\bar{\varepsilon}_{33}\frac{V}{h}cL. \end{aligned} \quad (11)$$

The currents flowing out of these electrodes are

$$\begin{aligned} I_{\mathrm{A}} &= -\dot{Q}_{\mathrm{A}} \\ &= (-i\omega)\left\{2s_{11}^{-1}d_{31}b(c+2h)[u_{3,1}(L) - u_{3,1}(0)] + 2\bar{\varepsilon}_{33}\frac{V}{h}bL\right\}, \\ I_{\mathrm{D}} &= -\dot{Q}_{\mathrm{D}} \\ &= (-i\omega)\left\{2s_{11}^{-1}d_{31}c(b+2h)[u_{2,1}(L) - u_{2,1}(0)] + 2\bar{\varepsilon}_{33}\frac{V}{h}cL\right\}. \end{aligned} \quad (12)$$

The output voltage and current are related by the following circuit condition:

$$I = I_{\mathrm{A}} + I_{\mathrm{D}} = \frac{4V}{Z_{\mathrm{L}}}. \quad (13)$$

This one-dimensional model for beam bending is known to be valid for long or thin beams [15].

IV. Solution

For time-harmonic motions, we use the usual complex notation:

$$\{u_2, u_3, V, Q, I\} = \mathrm{Re}\{\{U_2, U_3, \bar{V}, \bar{Q}, \bar{I}\}\exp(i\omega t)\}. \quad (14)$$

The general solutions to (8) can be written as

$$\begin{aligned} U_2 &= B_1\sin(\alpha_2 x_1) + B_2\cos(\alpha_2 x_1) + B_3\sinh(\alpha_2 x_1) \\ &\quad + B_4\cosh(\alpha_2 x_1), \\ U_3 &= C_1\sin(\alpha_3 x_1) + C_2\cos(\alpha_3 x_1) + C_3\sinh(\alpha_3 x_1) \\ &\quad + C_4\cosh(\alpha_3 x_1), \end{aligned} \quad (15)$$

where B_1 to B_4 and C_1 to C_4 are undetermined constants, and

$$\alpha_2 = \left(\frac{m\omega^2}{D_{22}}\right)^{1/4}, \quad \alpha_3 = \left(\frac{m\omega^2}{D_{33}}\right)^{1/4}. \quad (16)$$

Substituting (15) into the boundary conditions in (9) and (10) and the circuit condition in (13) yields the following nine linear algebraic equations for the nine unknowns of B_1 to B_4, C_1 to C_4, and $\bar{V}$:

$$\begin{aligned} &B_2 + B_4 = A\sin\theta, \\ &\alpha_2(B_1 + B_3) = 0, \\ &-D_{22}\alpha_2^2[-B_1\sin(\alpha_2 L) - B_2\cos(\alpha_2 L) + B_3\sinh(\alpha_2 L) \\ &\quad + B_4\cosh(\alpha_2 L)] + G_2\bar{V} = 0, \\ &D_{22}\alpha_2^3[-B_1\cos(\alpha_2 L) + B_2\sin(\alpha_2 L) + B_3\cosh(\alpha_2 L) \\ &\quad + B_4\sinh(\alpha_2 L)] = -m_0\omega^2[B_1\sin(\alpha_2 L) + B_2\cos(\alpha_2 L) \\ &\quad + B_3\sinh(\alpha_2 L) + B_4\cosh(\alpha_2 L)]. \end{aligned} \quad (17)$$

$$\begin{aligned} &C_2 + C_4 = A\cos\theta, \\ &\alpha_3(C_1 + C_3) = 0, \\ &-D_{33}\alpha_3^2[-C_1\sin(\alpha_3 L) - C_2\cos(\alpha_3 L) + C_3\sinh(\alpha_3 L) \\ &\quad + C_4\cosh(\alpha_3 L)] + G_3\bar{V} = 0, \\ &D_{33}\alpha_3^3[-C_1\cos(\alpha_3 L) + C_2\sin(\alpha_3 L) + C_3\cosh(\alpha_3 L) \\ &\quad + C_4\sinh(\alpha_2 L)] = -m_0\omega^2[C_1\sin(\alpha_3 L) + C_2\cos(\alpha_3 L) \\ &\quad + C_3\sinh(\alpha_3 L) + C_4\cosh(\alpha_3 L)]. \end{aligned} \quad (18)$$

$$\begin{aligned} \left(\frac{4}{Z_{\mathrm{L}}} + \frac{2}{Z_0}\right)\bar{V} &= -i\omega\{2s_{11}^{-1}d_{31}b(c+2h)\alpha_3[C_1\cos(\alpha_3 L) \\ &\quad - C_2\sin(\alpha_3 L) + C_3\cosh(\alpha_3 L) + C_4\sinh(\alpha_3 L)] \\ &\quad + 2s_{11}^{-1}d_{31}c(b+2h)\alpha_2[B_1\cos(\alpha_2 L) - B_2\sin(\alpha_2 L) \\ &\quad + B_3\cosh(\alpha_2 L) + B_4\sinh(\alpha_2 L)]\}. \end{aligned} \quad (19)$$

In (19), we have introduced

$$Z_0 = \frac{1}{i\omega C_0}, \quad C_0 = \frac{\bar{\varepsilon}_{33}(b+c)L}{h}. \quad (20)$$

Eqs. (17)–(19) are solved on a computer. With the complex notation, the output electrical power is given by [7]

$$P_2 = \frac{1}{2}[\bar{I}\bar{V}^* + \bar{I}^*\bar{V}], \quad (21)$$

where $*$ represents a complex conjugate. The power density, defined as the output power per unit volume, is

$$p_2 = \frac{P_2}{[4bc + 8(b+c)h]L}. \quad (22)$$

V. Numerical Results and Discussion

For the piezoelectric films, we used PZT-5H polarized ceramics with $\rho = 7500$ kg/m^3, $s_{11} = 16.5 \times 10^{-12}$ m^3/N, $d_{31} = -274 \times 10^{-12}$ C/N, and $\varepsilon_{11} = 3430\varepsilon_0$, where ε_0 is the electric permittivity of free space. The elastic beam is taken to be aluminum alloy with $\rho = 2700$ kg/m^3 and $E = 70$ GPa. In our numerical calculation, the real elastic constant s_{11} is replaced by $s_{11}(1 - iQ^{-1})$, where Q is the

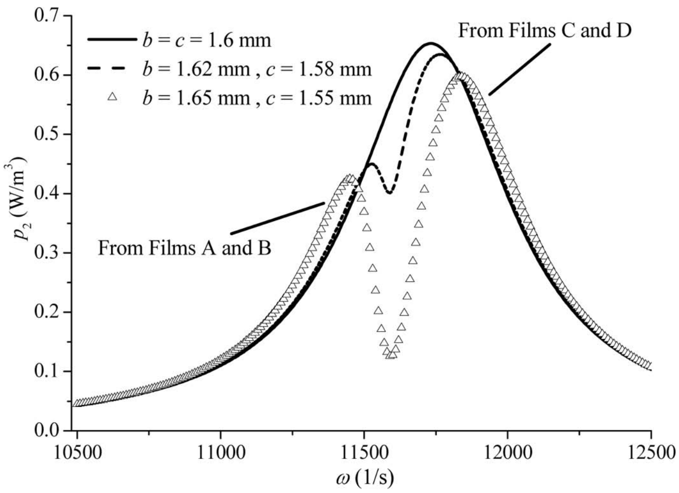

Fig. 2. Output power density versus driving frequency with an increased bandwidth.

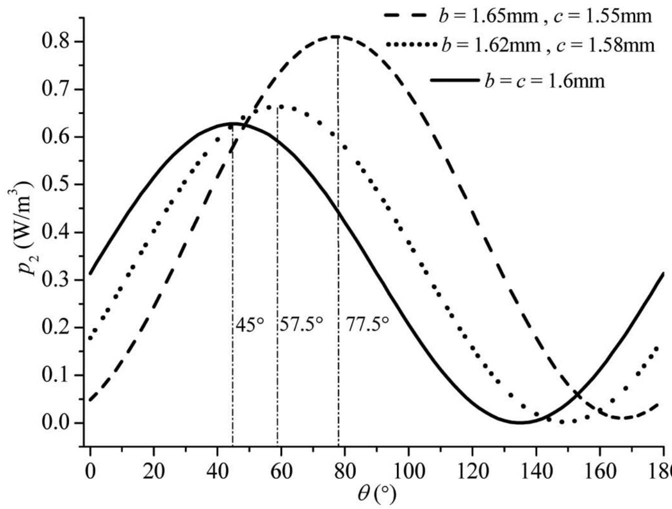

Fig. 3. Output power density versus θ.

quality factor of the material, a large and real number. For ceramics, Q is of the order of 10^2 to 10^3. We fix Q to be 10^2, which is chosen to be relatively small and is a representation of the damping of the whole structure. $L = 30$ mm, $Z_L = iZ_0$, and $A\omega^2 = 1$ ms^{-2} are fixed in the calculation.

Fig. 2 shows the output power density p_2 versus the driving frequency ω when $\theta = 45°$, $m_0 = 0.5$ mL, and $h = 0.8$ mm. The frequency range shown includes the frequencies of the lowest flexural modes in both the x_2 and x_3 directions. When the dimensions b and c of the beam cross section are sufficiently different, the resonant frequencies of the fundamental flexural modes in the x_2- and x_3-directions are also different. In this case, there are two separate, relatively narrow, peaks caused by separate resonances in the x_2- and x_3-directions (the line marked by small triangles). When b is larger than c, the flexural mode in the x_2-direction has a higher resonant frequency than the flexural mode in the x_3-direction. Hence, the peak on the right is from films C and D. Similarly, the peak on the left is from films A and B. When b and c are only slightly different, the two narrow peaks almost merge into one wide peak, showing an increased bandwidth (the dotted line). In the special case when $b = c$, the figure shows only a single wide peak (the solid line).

Fig. 3 shows the output power density versus the orientation of the cross section described by θ when $\omega = 11\,800$ Hz, $m_0 = 0.5$ mL, and $h = 0.8$ mm. First, we note that the output is periodic, with a period of π as expected. In the case of $b = c$, the maximal output happens when $\theta = 45°$, as expected in this case because the two output piezoelectric films at A and D are in tension or compression at the same time, producing charges of the same sign on the output electrode joining A and D. In the case of $b = c$ and $\theta = 135°$, the output is zero, as expected in this case because when one of A and D is in extension, the other is in compression, resulting in total charge cancellation from A and D on the output electrode joining A and D. When b and c are not equal and vary, the location of the maximal output is sensitive to the values of b and c. There also exits a θ for which there is zero output because of charge cancellation.

Fig. 4 shows the output power density versus the driving frequency ω for different h when $\theta = 45°$, $m_0 = 0.5$ mL, $b = 1.62$ mm, and $c = 1.58$ mm. When h increases, both the inertia and the bending stiffness of the structure increase. Because the bending stiffness is cubic in the dimension of the cross section, overall the increase of the bending stiffness dominates and the resonant frequencies increase. This makes it harder to drive the beam, and therefore the output power does not change much although there is more piezoelectric material in the structure when h increases.

Fig. 5 shows the output power density versus driving frequency ω for different m_0 when $\theta = 45°$, $h = 0.8$ mm, $b = 1.62$ mm, and $c = 1.58$ mm. When m_0 increases, the resonant frequencies become lower and the output power becomes larger, as expected.

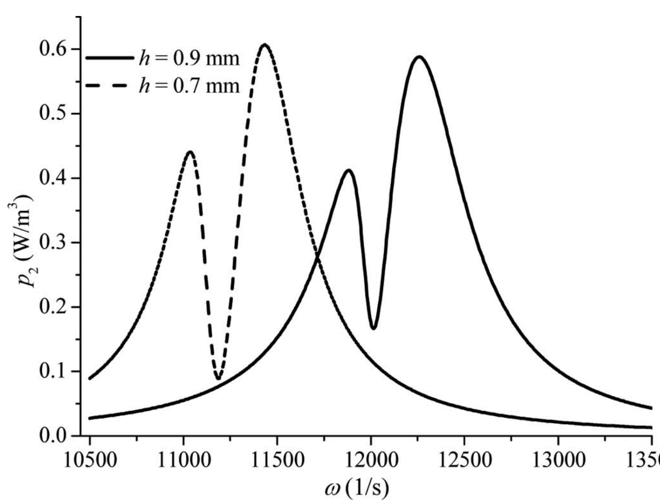

Fig. 4. Output power density versus driving frequency for different h.

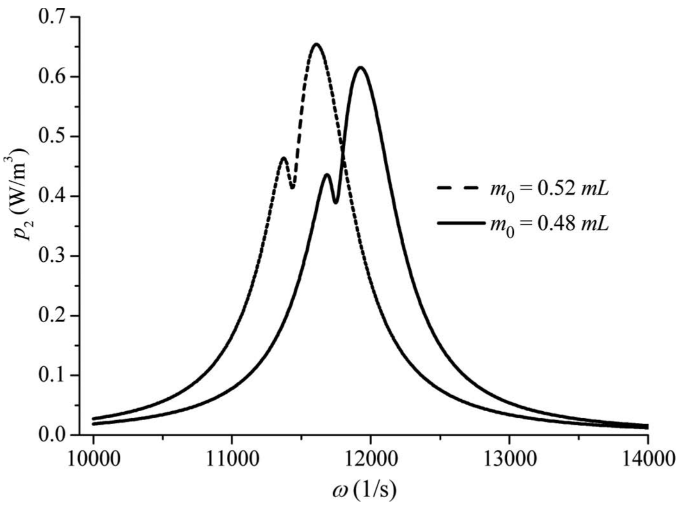

Fig. 5. Output power density versus driving frequency for different m_0.

VI. Conclusion

A single elastic beam with two pairs of piezoelectric films can operate as an energy harvester when the cross section is properly oriented and the electrodes are properly connected. Compared with the conventional bimorph energy harvester in flexural vibration in one direction, the frequency bandwidth through which energy can be harvested is increased in the proposed energy harvester with simultaneous flexural motions in two perpendicular directions.

References

[1] T. G. Engel, C. Keawboonchuay, and W. C. Nunnally, “Energy conversion and high power pulse production using miniature piezoelectric compressors,” *IEEE Trans. Plasma Sci.*, vol. 28, no. 5, pp. 1338–1341, 2000.

[2] G. W. Taylor, J. R. Burns, S. A. Kammann, W. B. Powers, and T. R. Welsh, “The energy harvesting eel: A small subsurface ocean/river power generator,” *IEEE J. Oceanic Eng.*, vol. 26, no. 4, pp. 539–547, 2001.

[3] S. Roundy, P. K. Write, and J. Rabaey, “A study of low level vibrations as a power source for wireless sensor nodes,” *Comput. Commun.*, vol. 26, no. 11, pp. 1131–1144, 2003.

[4] Y. S. Cho, Y. E. Pak, C. S. Han, and S. K. Ha, “Fiver-port equivalent electric circuit of piezoelectric bimorph beam,” *Sens. Actuators A*, vol. 84, no. 1–2, pp. 140–148, 2000.

[5] S. K. Ha, “Analysis of the asymmetric triple-layered piezoelectric bimorph using equivalent circuit models,” *J. Acoust. Soc. Am.*, vol. 110, no. 2, pp. 856–864, 2001.

[6] J. S. Yang, H. G. Zhou, Y. T. Hu, and Q. Jiang, “Performance of a piezoelectric harvester in thickness-stretch mode of a plate,” *IEEE Trans. Ultrason. Ferroelectr. Freq. Control*, vol. 52, no. 10, pp. 1872–1876, 2005.

[7] S. N. Jiang, X. F. Li, S. H. Guo, Y. T. Hu, J. S. Yang, and Q. Jiang, “Performance of a piezoelectric bimorph for scavenging vibration energy,” *Smart Mater. Struct.*, vol. 14, no. 4, pp. 769–774, 2005.

[8] S. R. Anton and H. A. Sodano, “A review of power harvesting using piezoelectric materials (2003–2006),” *Smart Mater. Struct.*, vol. 16, no. 3, pp. R1–R21, 2007.

[9] H. Xue, Y. T. Hu, and Q.-M. Wang, “Broadband piezoelectric energy harvesting devices using multiple bimorphs with different operating frequencies,” *IEEE Trans. Ultrason. Ferroelectr. Freq. Control*, vol. 55, no. 9, pp. 2104–2108, 2008.

[10] Z. T. Yang and J. S. Yang, “Connected vibrating piezoelectric bimorph beams as a wide-band piezoelectric power harvester,” *J. Intell. Mater. Syst. Struct.*, vol. 20, no. 5, pp. 569–574, 2009.

[11] L. H. Tang, Y. W. Yang, and C. K. Soh, “Toward broadband vibration-based energy harvesting,” *J. Intell. Mater. Syst. Struct.*, vol. 21, no. 18, pp. 1867–1897, 2010.

[12] J. S. Yang and H. Y. Fang, “Analysis of a rotating elastic beam with piezoelectric films as an angular rate sensor,” *IEEE Trans. Ultrason. Ferroelectr. Freq. Control*, vol. 49, no. 6, pp. 798–804, 2002.

[13] J. S. Yang, “Equations for the extension and flexure of a piezoelectric beam with rectangular cross section and applications,” *Int. J. Appl. Electromagn. Mech.*, vol. 9, no. 4, pp. 409–420, 1998.

[14] J. S. Yang, H. Y. Fang, and Q. Jiang, “Analysis of a ceramic bimorph piezoelectric gyroscope,” *Int. J. Appl. Electromagn. Mech.*, vol. 10, no. 6, pp. 459–473, 1999.

[15] R. D. Mindlin, “Low frequency vibrations of elastic bars,” *Int. J. Solids Struct.*, vol. 12, no. 1, pp. 27–49, 1976.